PROCEEDINGS OF SCIENCE

Recent diboson and polarization measurements at CMS

Saptaparna Bhattacharya* **on behalf of the CMS Collaboration**

Wayne State University,
666 W Hancock Street, Detroit MI 48201, United States of America

E-mail: saptaparna.bhattacharya@cern.ch

Over the course Run 1 and Run 2 of the Large Hadron Collider (LHC), more than 150 fb^{-1} of data has been collected by the Compact Muon Solenoid (CMS) experiment at the Large Hadron Collider. This large dataset has facilitated the precision measurement of several Standard Model (SM) processes. Diboson processes, where two gauge bosons are simultaneously produced in one LHC collision event, fall within the category of processes that can be measured with precision. These processes feature the trilinear gauge coupling and provide important tests of the non-Abelian gauge structure of the SM. The measurement of properties of the gauge boson, such as the polarization, can be carried out with these processes. The first measurement of longitudinally polarized W-bosons was performed by the CMS Collaboration in the study of the fully leptonic decays of the gauge bosons in a WZ process. The novel technique of tagging protons using the precision proton spectrometer enables the precision studies of dibosons produced in photon-induced processes, allowing unique access to the quartic coupling between photons and gauge bosons. Finally, a comprehensive measurement of the polarization of the τ lepton in a final state where the Z-boson decays to pairs of τ leptons is presented. The precision on the measured value of the τ polarization surpasses previous measurements at the LHC.

The Eleventh Annual Conference on Large Hadron Collider Physics (LHCP2023)
22-26 May 2023
Belgrade, Serbia

*Speaker

PoS(LHCP2023)144

1. Introduction

In this document, several recent diboson cross section and polarization measurements are presented. In section 1.1, the first differential measurement in the ZZ process, where each Z boson decays to a pair of leptons, with the full Run 2 dataset of the LHC amounting to 137 fb^{-1} is discussed. In section 1.2, the pair production of gauge bosons in photon-initiated processes is described. In sections 1.3 and 1.4, recent polarization measurements in the WZ process and the τ polarization in the $Z \rightarrow \tau\tau$ process are presented, the former reporting the first measurement of longitudinally polarized W bosons.

1.1 Measurement of ZZ production in 4 lepton final state [1]

In the SM, the ZZ process occurs via the t and u-channel modes of production. The s-channel production of ZZ bosons is forbidden in the SM and the loop effects in this process contribute up to 10% of the total cross section, making this an interesting process for the study of the SM and potential signs of beyond the SM (BSM) physics. The inclusive cross section has been studied in detail previously by both CMS and ALTAS Collaborations ([2–6]). The first measurement of the differential cross sections as a function of the (a) number of jets and the transverse momentum (p_T) and pseudorapidity ($|\eta|$) of the jets (b) the invariant mass of the highest p_T and the second highest p_T jets (c) The difference in η ($\Delta|\eta|$) of the highest p_T and the second highest p_T jets and the (d) invariant mass of the four lepton system ($m_{4\ell}$) as a function of different jet multiplicities is reported. The results are compared with the state-of-the-art next-to-next-to-leading order (NNLO) and parton shower (PS) predictions using MiNNLO$_{PS}$ [7, 8]. As shown in the second panel of Fig. 1, the predictions over-estimate the data and the largest discrepancy is seen for the highest p_T jet, for cases where the p_T < 100 GeV. The shape of the distributions is well described by the Monte Carlo (MC) simulations and the discrepancy arises from the normalization of the predictions. In the distribution of the m_{4l} shown in the first panel of Fig. 1, the predictions agree with data in an event category with no jets, while the discrepancy in the normalization is evident in the event category with one jet (second panel of Fig. 1).

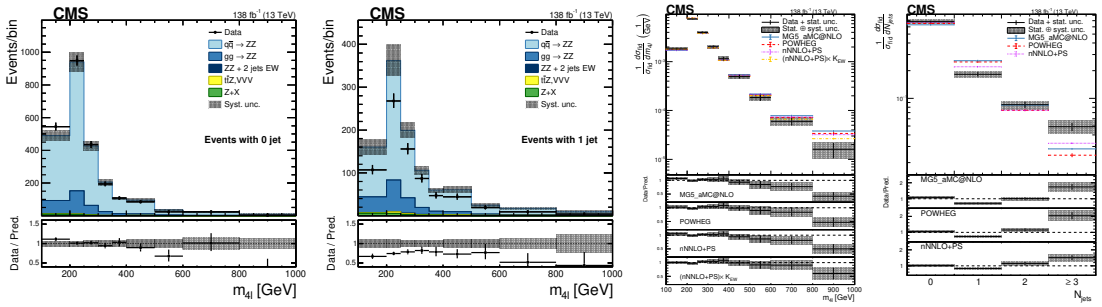

Figure 1: First panel: The distribution of the invariant mass of four leptons ($m_{4\ell}$) in an event category with no jets. Second panel: The $m_{4\ell}$ distribution in an event category with one jet. Third and fourth panel: Unfolded distributions as function of the mass of the four leptons and the number of jets [1].

The highest source of theoretical uncertainty in this analysis arises from the variation of the renormalization and factorization scales. This large uncertainty could indicate that higher order corrections exceeding the sample accuracy (next-to-leading order (NLO)) are at play. Therefore the impact of the inclusion of higher order calculations and comparison with MiNNLO$_{PS}$ was carried out after the distributions were unfolded to factor out experimental effects. The differential cross sections were normalized to the fiducial cross sections, where the fiducial requirement is that both Z-candidates in the event be on mass shell ($60 < m_{Z_1,Z_2} < 120$). The cross sections of the samples are normalized to the cross sections calculated at NNLO for $q\bar{q} \rightarrow ZZ$ [9] (K factor of 1.1) and at NLO in QCD for $gg \rightarrow ZZ$ [10] (K factor of 1.7). The unfolded distributions are shown in last two panels of Fig. 1 where the discrepancy between data and simulations are better understood when detailed comparisons are performed with several event generators such as, Madgraph5_aMC@NLO [11] (for the quark initiated process $q\bar{q} \rightarrow ZZ$) with MCFM [12] (for the gluon initiated process $gg \rightarrow ZZ$) and POWHEG [13–16] (for the Higgs contribution to the signal, $H \rightarrow ZZ$) in dark blue color. Another comparison features POWHEG (for the quark initiated process $q\bar{q} \rightarrow ZZ$) with MCFM (for the gluon initiated process $gg \rightarrow ZZ$) and POWHEG (for the Higgs contribution to the signal,

$H \to ZZ$ in red color. In both of the above processes electroweak corrections were taken into account using the Madgraph5_aMC@NLO event generator. The pink curve shows the comparison with MiNNLO$_{PS}$, while the yellow curve shows the case where electroweak corrections at NLO are incorporated in the MiNNLO$_{PS}$ prediction and shows superior agreement of the simulations with data.

1.2 Search for exclusive $\gamma\gamma \to W^+W^-$ and $\gamma\gamma \to ZZ$ production with jets and forward protons [17]

The production of a pair of gauge bosons in a photon-induced initial state, which allows unique access to the quartic photon and W or Z boson vertex, can be studied at the LHC. The precision proton spectrometer (PPS) can tag both protons in the event enabling searches for anomalous high-mass $\gamma\gamma \to WW$ and $\gamma\gamma \to ZZ$ contributions from new physics operators of higher order. The a_0^W/Λ^2 and a_C^W/Λ^2 (a_0^Z/Λ^2 and a_C^Z/Λ^2) operators, where Λ is the scale of new physics, will modify the $\gamma\gamma \to WW$ ($\gamma\gamma \to ZZ$) coupling [18, 19]. The PPS is a system of near-beam tracking and timing detectors, located in Roman pots (RPs) at about 200 m from the CMS interaction point. These devices are movable and can be brought within a few mm of the beam. The protons are matched to the jets based on certain variables: 1 - m(VV)/m(pp) and y(pp) − y(VV), where m(VV) and y(VV) represent the invariant mass and rapidity of the WW or ZZ system, reconstructed from boosted jets. The variables m(pp) and y(pp) are calculated as: $m(\mathrm{pp}) = \sqrt{s}\sqrt{\xi_{\mathrm{p1}}\xi_{\mathrm{p2}}}$ and $y(\mathrm{pp}) = -\frac{1}{2}\ln\left(\frac{\xi_{\mathrm{p1}}}{\xi_{\mathrm{p2}}}\right)$, where ξ is the proton fractional momentum loss $((p_{\mathrm{nom}} - p)/p_{\mathrm{nom}})$ between the nominal beam momentum and the scattered proton momentum. The constraints on anomalous interactions obtained with the novel usage of proton tagging leads to at least 15 to 20 times more stringent limits than previous results. Event yields with nominal BSM scenarios are shown in the first panel of Fig. 2, where the regions "δ" and "o" are defined on the y(pp) − y(VV) versus 1 - m(VV)/m(pp) plane. The region "δ" contains events where both protons are correctly associated with jets and region "o" picks up the cases where one of the signal protons is missed.

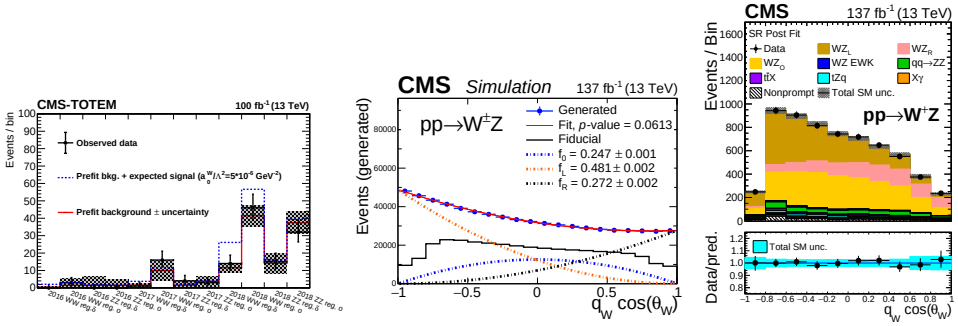

Figure 2: First: The event yields corresponding to 100 fb^{-1} for various event categories with specific requirements on the relative rapidity of the gauge bosons with respect to the protons and the ratio of the masses of the diboson system with respect to the proton. The analysis is performed using data collected with forward proton detectors in place and corresponding to 100 fb^{-1} [17]. Second: Distribution of the cosine of the polarization angle in the helicity frame. The blue points shown the predictions from Monte Carlo (MC) simulations in the total phase space [20]. The solid red line shows the best quadratic fit to the MC prediction, and the different dashed lines each show the polarization components. The solid black line shows the distribution of the same variable restricted to the fiducial phase space, showing how kinematic requirements break the quadratic dependence of the differential cross section. Third: Distribution of the cosine of the polarization angle of the W boson for the positive final-state charge after the corresponding fit [20].

1.3 Measurement of the WZ process [20]

The process of WZ production is sensitive to the parton distribution function of u and d quarks and is relatively unaffected by the gluon. The high WZ cross section makes it the dominant process that can be studied in the trilepton final state, a final state with low background rates. The ratio of $\frac{W^+Z}{W^-Z}$ cross section is one of the most precisely measurable quantities, with an uncertainty of 2.5%. This analysis constitutes the first measurement of longitudinally polarized W bosons in the WZ process. The W (Z) polarization angle θ_{W} (θ_{Z}) is defined as the angular distance between the momenta of the W (Z) boson and the (negatively) charged lepton from its primary decay. The differential WZ cross section with respect to the cosine of the polarization angle, at Born level, can be directly related to the fraction of transversely (left L or right R) and longitudinally (0) polarized bosons through the following analytic functions [21, 22]: $\frac{1}{\sigma}\frac{d\sigma}{d\cos\theta_{\mathrm{W}^\pm}} = \frac{3}{8}\left[(1 \mp \cos(\theta_{W^\pm}))^2 f_L^{\mathrm{W}} + (1 \pm \cos(\theta_{W^\pm}))^2 f_R^{\mathrm{W}} + 2\sin^2(\theta_{W^\pm}) f_0^{\mathrm{W}}\right]$, and

$\frac{d\sigma}{\sigma d\cos\theta_Z} = \frac{3}{8}\left[(1+\cos^2(\theta_Z) - 2c\cos(\theta_Z))f_L^Z + (1+\cos^2(\theta_Z) + 2c\cos(\theta_Z))f_R^Z + 2\sin^2(\theta_Z)f_0^Z\right]$ where f_L^W, f_R^W, and f_0^W (f_L^Z, f_R^Z, and f_0^Z) are observables referred to as polarization fractions. The constant c appears due to the coupling of the Z boson to fermions of different chiralities, $c = \frac{c_L^2 - c_R^2}{c_L^2 + c_R^2}$, where c_L=-(1/2) + $\sin^2(\theta_{\text{eff}})$ and c_R=$\sin^2(\theta_{\text{eff}})$ are the vector and axial-vector couplings of the Z boson to leptons and θ_{eff} is the effective weak mixing angle. The polarization state of massive vector bosons is the projection of the spin over the momentum and is therefore intrinsically frame-dependent. The analytic functions described above are applicable in cases where no kinematic requirements are applied to the decay products of the W and Z bosons, a nonrealistic condition when measurements are performed with data. To circumvent this issue, the signal is separated into three polarization components (left, right, and longitudinal) based on generator-level information and events in the sample are then weighted by the expected $\cos\theta_W$ ($\cos\theta_Z$) distributions that exhibit quadratic dependence based on the corresponding polarization state. In the second panel of Fig. 2, the polarization fractions needed to perform this weighting (extracted from an analytical fit) are shown. The distribution of the cosine of the polarization angle for W^+Z after the extraction of the polarization fractions is shown in the last panel of Fig 2, where the fractions have to satisfy $f_L + f_R + f_0 = 1$.

1.4 Tau (τ) polarization in Z-boson decays [23]

The polarization of τ leptons is measured in $Z \to \tau\tau$ events. The differential cross section of the $q\bar{q} \to Z \to \tau^+\tau^-$ in the lowest order is expressed as:

$$\frac{d\sigma}{d\cos\theta_\tau} = F_0(\hat{s})(1+\cos^2\theta_\tau) + 2F_1(\hat{s})\cos\theta_\tau - \lambda_\tau[F_2(\hat{s})(1+\cos^2\theta_\tau) + 2F_3(\hat{s})\cos\theta_\tau]$$

The forward-backward asymmetry is defined in terms of F_1 and F_0, the polarization is defined in terms of F_2 and F_0, while the forward-backward polarization asymmetry is expressed in terms of F_3 and F_0, and θ_τ is the scattering angle of the τ^- with respect to the quark momentum in the rest frame of the Z boson as shown in the left panel of Fig. 3. The sign of the helicity is denoted by λ_τ and $\hat{s}$ is the partonic center-of-mass energy. The equation is simplified when $\sqrt{s} = M_Z$. In the decay of the τ leptons, the angle θ as shown in the right panel of Fig. 3 is defined as the angle between the boost direction of the τ lepton projected onto the τ lepton rest frame and the direction of momentum of the hadron. Several such spin sensitive angles are defined and the collective angular information is combined into a unique one-dimensional optimal variable conceptually analogous to a polarimetric vector. The differential width of any decay of a polarized τ^- lepton in its rest frame (assuming spin aligns with the momentum) is given by [24–26]: $\frac{d\Gamma}{d\cos\zeta_h} \propto \frac{1}{2}(1 + \mathcal{P}_\tau\cos\zeta_h)$, where $\mathcal{P}_\tau$ is the τ^- lepton polarization for a given τ^- lepton decay and ζ_h is the angle between the space-like polarimetric vector $\vec{h}_\tau$ and $\vec{n}_\tau$ (unit vector pointing in the τ boost direction). The measured τ^- lepton polarization at the Z-boson mass pole is $\mathcal{P}_\tau(Z)$ = -0.144 ± 0.006 (stat.) ± 0.014 (syst.) and is in good agreement with the measurement of the τ lepton asymmetry parameter at LEP. The τ polarization is a function of the ratio of the vector to axial-vector couplings of the τ leptons and is, therefore, related to the effective weak mixing angle $\sin^2\theta_W^{\text{eff}}$, which is measured as 0.2319 ± 0.0008 (stat.) ± 0.0018 (syst.) and is in good agreement with measurements at e^+e^- colliders.

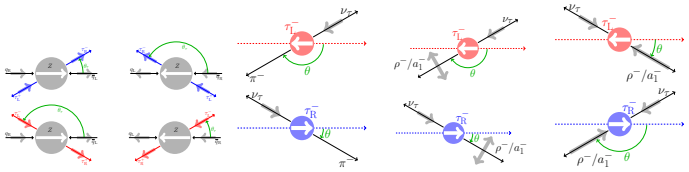

Figure 3: Left panel: Helicity states of incoming quarks and outgoing τ leptons. The thin arrows show direction of movement, while the thick arrows show helicity. Right panel: The decay angles of the τ in $\tau \to h\nu$ decays [23].

2. Conclusion

Several diboson analyses, namely, ZZ, WZ and photon-initiated processes with novel analyses methods, are presented. A comprehensive exploration of final states with a τ lepton arising from the decay of Z bosons is reported. Diboson physics is being performed at the precision realm enabling stringent tests of the electroweak gauge sector of the Standard Model of Particle Physics.

References

[1] CMS Collaboration, Measurement of the differential ZZ+jets production cross sections in pp collisions at $\sqrt{s}$ = 13 TeV, arXiv:2404.02711 [hep-ex]

[2] CMS Collaboration, Measurement of the ZZ production cross section and search for anomalous couplings in 2 l2l' Final States in pp Collisions at $\sqrt{s}$ = 7 TeV, JHEP 01 (2013) 063

[3] CMS Collaboration, Measurement of the $pp \to ZZ$ production cross section and constraints on anomalous triple gauge couplings in four-lepton final states at $\sqrt{s}$ = 8 TeV, Phys. Lett. B 740 (2015) 250

[4] ATLAS Collaboration, Measurement of ZZ production in pp collisions at $\sqrt{s}$ = 7 TeV and limits on anomalous ZZZ and $ZZ\gamma$ couplings with the ATLAS detector, *Journal of High Energy Physics*, JHEP 03 (2013) 128, arXiv:1211.6096 [hep-ex]

[5] ATLAS Collaboration, Measurements of four-lepton production in pp collisions at $\sqrt{s}$ = 8 TeV with the ATLAS detector, https://doi.org/10.1016/j.physletb.2015.12.048, arXiv:1509.07844 [hep-ex]

[6] ATLAS Collaboration, $ZZ \to \ell^+\ell^-\ell'^+\ell'^-$ cross-section measurements and search for anomalous triple gauge couplings in 13 TeV pp collisions with the ATLAS detector, Phys. Rev. D 97, 032005 (2018), arXiv:1709.07703 [hep-ex]

[7] Luca Buonocore, Gabriël Koole, Daniele Lombardi, Luca Rottoli, Marius Wiesemann, Giulia Zanderighi, ZZ production at nNNLO+PS with MiNNLO$_{PS}$, JHEP 05 (2020) 143,, arXiv:2108.05337

[8] Pier Francesco Monni, Paolo Nason, Emanuele Re, Marius Wiesemann, Giulia Zanderighi, MiNNLO$_{PS}$: a new method to match NNLO QCD to parton showers, *Journal of High Energy Physics*, JHEP 05 (2020) 143, arXiv:1908.06987 [hep-ex]

[9] F. Cascioli, T. Gehrmann, M. Grazzini, S. Kallweit, P. Maierhöfer, A. von Manteuffel, S. Pozzorini, D. Rathlev, L. Tancredi, E. Weihs, ZZ production at hadron colliders in NNLO QCD, PLB 735 (2014) 311, arXiv:1405.2219 [hep-ph]

[10] F. Caola, K. Melnikov, R. Roïtsch, and L. Tancredi, QCD corrections to ZZ production in gluon fusion at the LH, Phys. Rev. D 92 (2015) 094028 arXiv:1509.06734 [hep-ph]

[11] J. Alwall, R. Frederix, S. Frixione, V. Hirschi, F. Maltoni, O. Mattelaer, H.-S. Shao, T. Stelzer, P. Torrielli, M. Zaro, The automated computation of tree-level and next-to-leading order differential cross sections, and their matching to parton shower simulations, JHEP 07 (2014) 079, arXiv:1405.0301 [hep-ph]

[12] J. M. Campbell and R. K. Ellis, MCFM for the Tevatron and the LHC, *Nucl. Phys. B Proc. Suppl.* 10 (2010) 205, arXiv:1007.3492 [hep-ph]

[13] S. Alioli, P. Nason, C. Oleari, and E. Re, A general framework for implementing NLO calculations in shower Monte Carlo programs: the POWHEG BOX, JHEP 06 (2010) 043, arXiv:1002.2581 [hep-ph]

[14] S. Alioli, P. Nason, C. Oleari, and E. Re, NLO vector-boson production matched with shower in POWHEG, JHEP 07 (2008) 060, arXiv:0805.4802 [hep-ph].

[15] P. Nason, A new method for combining NLO QCD with shower Monte Carlo algorithms, JHEP 11 (2004) 040, arXiv:hep-ph/0409146.

[16] S. Frixione, P. Nason, and C. Oleari, Matching NLO QCD computations with parton shower simulations: the POWHEG method, JHEP 11 (2007) 070, arXiv:0709.2092 [hep-ph]

[17] CMS Collaboration, Search for high-mass exclusive $\gamma\gamma \to WW$ and $\gamma\gamma \to ZZ$ production in proton-proton collisions at $\sqrt{s}$ = 13 TeV, JHEP 07 (2023) 229

[18] G. Bèlanger, F. Boudjema, Y. Kurihara, D. Perret-Gallix, and A. Semenov, Bosonic quartic couplings at LEP-2, Eur. Phys. J. C 13 (2000) 283, arXiv:hep-ph/9908254

[19] G. Bèlanger, F. Boudjema, $\gamma\gamma \to W^+W^-$ and $\gamma\gamma \to ZZ$ as tests of novel quartic couplings, Phys.Lett.B 288 (1992) 210-220

[20] CMS Collaboration, Measurement of the inclusive and differential WZ production cross sections, polarization angles, and triple gauge couplings in pp collisions at $\sqrt{s}$ = 13 TeV, JHEP 07 (2022) 032

[21] J. A. Aguilar-Saavedra and J. Bernabeu, Breaking down the entire W boson spin observables from its decay, Phys. Rev. D 93 (2016) 011301, arXiv:1508.04592 [hep-ph]

[22] J. A. Aguilar-Saavedra, J. Bernabeu, V. A. Mitsou, and A. Segarra,, The Z boson spin observables as messengers of new physics, Eur. Phys. J. C 77 (2017) 234, arXiv:1701.03115 [hep-ph]

[23] CMS Collaboration, Measurement of the τ polarization in Z boson decays in proton-proton collisions at $\sqrt{s}$ = 13 TeV, JHEP 01 (2024) 101

[24] S. Jadach, Z. Wąs, R. Decker, and J. H. Kühn, The τ decay library TAUOLA, version 2.4, Comput. Phys. Commun. 76 (1993) 361

[25] Y.-S. Tsai, Decay correlations of heavy leptons in $e^+e^- \to \ell^+\ell^-$, Phys. Rev. D 4 (1971) 2821

[26] V. Cherepanov and W. Lohmann, Methods for a measurement of τ polarization asymmetry in the decay $Z \to \tau\tau$ at LHC and determination of the effective weak mixing angle, arXiv:1805.10552 [hep-ph]

PoS(LHCP2023)144